arXiv:nucl-ex/0509041v4 17 Oct 2005

NA49 results on hadron production: indications of the onset of deconfinement ?

Benjamin Lungwitz for the NA49 collaboration[0]

Institut für Kernphysik, Johann-Wolfgang Goethe Universität Frankfurt,
Max-von-Laue-Str. 1, 60438 Frankfurt am Main

C. Alt[9], T. Anticic[21], B. Baatar[8],D. Barna[4], J. Bartke[6], L. Betev[10], H. Białkowska[19], C. Blume[9], B. Boimska[19], M. Botje[1], J. Bracinik[3], R. Bramm[9], P. Bunčić[10], V. Cerny[3], P. Christakoglou[2], O. Chvala[14], J.G. Cramer[16], P. Csató[4], P. Dinkelaker[9], V. Eckardt[13], D. Flierl[9], Z. Fodor[4], P. Foka[7], V. Friese[7], J. Gál[4], M. Gaździcki[9,11], V. Genchev[18], G. Georgopoulos[2], E. Gładysz[6], K. Grebieszkow[20], S. Hegyi[4], C. Höhne[7], K. Kadija[21], A. Karev[13], M. Kliemant[9], S. Kniege[9], V.I. Kolesnikov[8], E. Kornas[6], R. Korus[11], M. Kowalski[6], I. Kraus[7], M. Kreps[3], A. Laszlo[4], M. van Leeuwen[1], P. Lévai[4], L. Litov[17], B. Lungwitz[9], M. Makariev[17], A.I. Malakhov[8], M. Mateev[17], G.L. Melkumov[8], A. Mischke[1], M. Mitrovski[9], J. Molnár[4], St. Mrówczyński[11], V. Nicolic[21], G. Pálla[4], A.D. Panagiotou[2], D. Panayotov[17], A. Petridis[2], M. Pikna[3], D. Prindle[16], F. Pühlhofer[12], R. Renfordt[9], C. Roland[5], G. Roland[5], M. Rybczyński[11], A. Rybicki[6,10], A. Sandoval[7], N. Schmitz[13], T. Schuster[9], P. Seyboth[13], F. Siklér[4], B. Sitar[3], E. Skrzypczak[20], G. Stefanek[11], R. Stock[9], C. Strabel[9], H. Ströbele[9], T. Susa[21], I. Szentpétery[4], J. Sziklai[4], P. Szymanski[10,19], V. Trubnikov[19], D. Varga[4,10], M. Vassiliou[2], G.I. Veres[4,5], G. Vesztergombi[4], D. Vranić[7], A. Wetzler[9], Z. Włodarczyk[11] I.K. Yoo[15], J. Zimányi[4]

[1]NIKHEF, Amsterdam, Netherlands.
[2]Department of Physics, University of Athens, Athens, Greece.
[3]Comenius University, Bratislava, Slovakia.
[4]KFKI Research Institute for Particle and Nuclear Physics, Budapest, Hungary.
[5]MIT, Cambridge, USA.
[6]Institute of Nuclear Physics, Cracow, Poland.
[7]Gesellschaft für Schwerionenforschung (GSI), Darmstadt, Germany.
[8]Joint Institute for Nuclear Research, Dubna, Russia.
[9]Fachbereich Physik der Universität, Frankfurt, Germany.
[10]CERN, Geneva, Switzerland.
[11]Institute of Physics Świ etokrzyska Academy, Kielce, Poland.
[12]Fachbereich Physik der Universität, Marburg, Germany.
[13]Max-Planck-Institut für Physik, Munich, Germany.
[14]Institute of Particle and Nuclear Physics, Charles University, Prague, Czech Republic.

---

[0] presented at the XXXVth International Symposium on Multiparticle Dynamics 2005.

[15]Department of Physics, Pusan National University, Pusan, Republic of Korea.
[16]Nuclear Physics Laboratory, University of Washington, Seattle, WA, USA.
[17]Atomic Physics Department, Sofia University St. Kliment Ohridski, Sofia, Bulgaria.
[18]Institute for Nuclear Research and Nuclear Energy, Sofia, Bulgaria.
[19]Institute for Nuclear Studies, Warsaw, Poland.
[20]Institute for Experimental Physics, University of Warsaw, Warsaw, Poland.
[21]Rudjer Boskovic Institute, Zagreb, Croatia.

Abstract. The NA49 experiment at the CERN SPS measured the energy and system size dependence of particle production in A+A collisions. A change of the energy dependence of several hadron production properties at low SPS energies is observed which suggests a scenario requiring the onset of deconfinement.

INTRODUCTION

In heavy ion interactions at sufficiently high collision energy the creation of a deconfined state of matter, the quark gluon plasma (QGP), is expected [1, 2]. At RHIC and top SPS energies the energy density of the fireball in the early stage was estimated to be large enough to create QGP. In contrast at low AGS energies the maximum energy density is probably too low for the creation of deconfined matter. In order to look for the onset of deconfinement the NA49 experiment at the CERN SPS studied the hadronic final state of Pb+Pb collisions in the energy range 20*A* - 158*A* GeV.
In addition to the energy scan program, NA49 also measured the dependence of hadron production properties on the size of the colliding nuclei and the centrality of collisions.

THE NA49 EXPERIMENT

The NA49 detector system [3] is a large acceptance fixed target hadron spectrometer. Its main devices are four large time projection chambers (TPCs). Two of them, called vertex TPCs, are located in two superconducting dipole magnets. The other two TPCs are installed behind the magnets left and right of the beam line allowing precise particle tracking in the high density region of heavy ion collisions.
The accuracy of momentum determination is $\Delta p/p^2 \approx (0.3-7)\cdot 10^{-4}$ (GeV/c)$^{-1}$.

The measurement of the energy loss dE/dx allows identification of pions, protons, kaons and electrons for momenta $p > 4$ GeV/c. The NA49 experiment is equipped with two time of flight walls which, together with the energy loss measurement, allow a good separation of the particle species at midrapidity. Decaying particles can be identified with a good precision via the reconstruction of the decay vertex and / or the invariant mass method.

The downstream veto calorimeter allows a determination of the centrality of a collision by measuring the energy in the projectile spectator region. This measure of centrality is independent of the multiplicity of produced particles which is important in a study of multiplicity fluctuations.

A large variety of different colliding systems was studied. Beams of p and Pb are available at the CERN SPS directly, C and Si beams were produced via fragmentation of the primary Pb beam. Targets of liquid hydrogen or solid foils of different materials were used.

In this paper results of the energy scan, which covers Pb+Pb collisions at 20*A*, 30*A*, 40*A*, 80*A* and 158*A* GeV, and results of the system size scan at 40*A* and 158*A* GeV are shown. The data should be considered preliminary unless a reference to the corresponding publication is given.

RESULTS

Pions:

Most of the produced particles are pions and thus they carry most of the entropy produced in the collision.

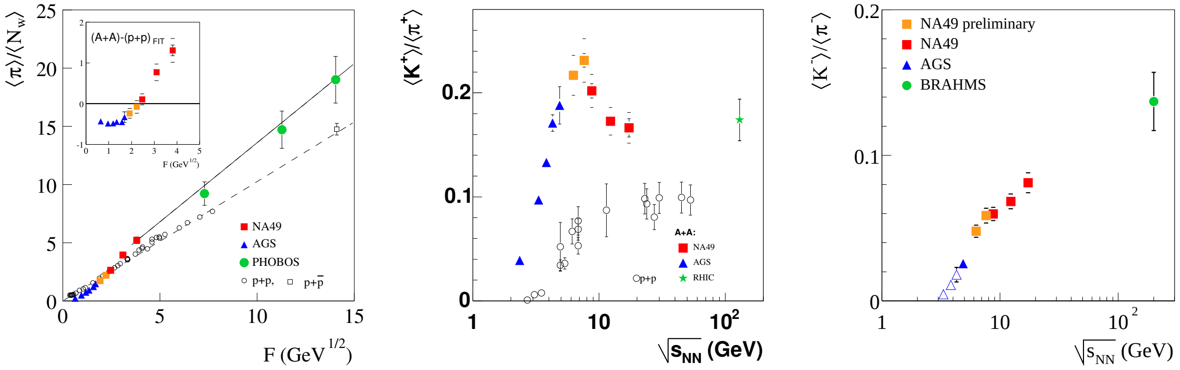

FIGURE 1. Energy dependence of pion multiplicity $\langle\pi\rangle$ to the nubmer of wounded nucleons $\langle N_W\rangle$ [4] (left), of the $\langle K^+\rangle / \langle\pi^+\rangle$ ratio (middle) and the $\langle K^-\rangle / \langle\pi^-\rangle$ ratio [4] (right) in Pb+Pb (Au+Au) (full symbols) and p+p($\bar{\text{p}}$) (open symbols) collisions.

Figure 1 shows the pion yield per wounded nucleon in central Pb+Pb (Au+Au) collisions and p+p interactions as a function of the Fermi variable $F = \left(\sqrt{s_{NN}} - 2m_N\right)^{3/4} / \left(\sqrt{s_{NN}}\right)^{1/4} \approx \sqrt{\sqrt{s_{NN}}}$. The ratio $\langle\pi\rangle / \langle N_W\rangle$ rises linearly with F for p+p interactions. For heavy ion collisions at low energies $\langle\pi\rangle / \langle N_W\rangle$ is smaller than for p+p by a constant amount which may be attributed [5] to pion absorption in the hadronic medium. At low SPS energies the pion multiplicity in Pb+Pb collisions starts to increase faster with energy than in p+p interactions. This enhancement of pion production may indicate an increase of the number of degrees of freedom in the QGP phase and suggests the onset of deconfinement at low SPS energies.

The system size dependence of pion production for various energies is shown in figure 2. Both the suppression at low energies and the enhancement at high energies start already in small systems.

Kaons:

Strangeness is a very interesting observable because it is expected to be produced differently in a hadron gas and in the QGP. At SPS energies s-quarks are carried mainly

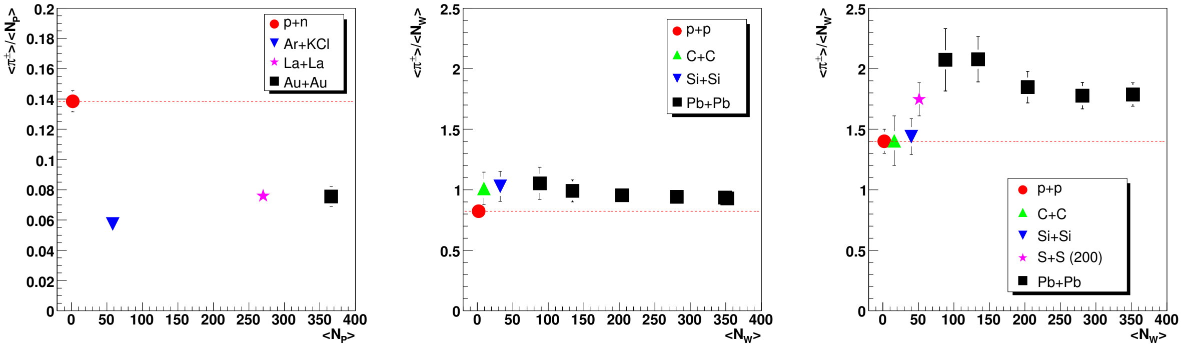

FIGURE 2. System size dependence of pion yield for 2*A* GeV [6, 7] (left), 40*A* GeV [8] (middle) and 158*A* GeV [9, 10] (right).

by Λs and anti-kaons, while most $\bar{s}$-quarks are carried by kaons. Therefore the K^+ meson multiplicity is approximately equal to half to the total number of $\bar{s}$ (and therefore also s) quarks produced in the collision. In order to take out the influence of center of mass energy on particle production the strange hadron yields are divided by the number of pions.

The energy dependence of the $\langle K^+\rangle / \langle \pi^+\rangle$ ratio shows (figure 1) the famous "horn" which can not be reproduced by hadron gas models assuming $\gamma_S = 1$ or string hadronic models. The increase of the $\langle K^-\rangle / \langle \pi^-\rangle$ ratio slows down at low SPS energies. Both features are consistent with a model assuming a first order phase transition [5] in which they are explained by a lower fraction of strange to non-strange degrees of freedom in the QGP than in the hadron gas.

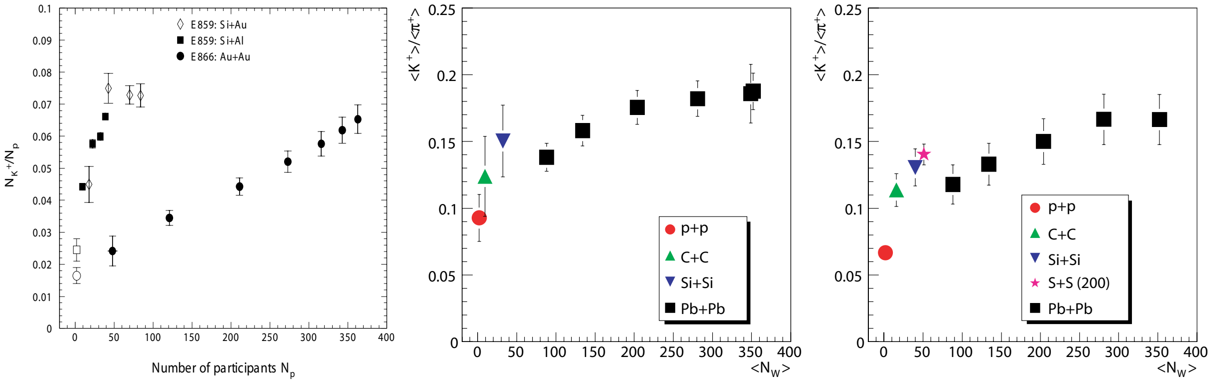

FIGURE 3. System size dependence of the $\langle K^+\rangle / \langle \pi^+\rangle$ ratio at 5*A* GeV [11], 40*A* GeV [8] and 158*A* GeV [9, 10].

For central collisions the $\langle K^+\rangle / \langle \pi^+\rangle$ ratio rises quickly with system size for all energies as shown in figure 3. This effect can be attributed to the strong volume dependence of relative strangeness production, in statistical models known as canonical strangeness suppression [9, 12].

The relative kaon production increases with centrality of the collision, the increase is faster and it saturates earlier for higher energies.

The number of wounded (or participant) nucleons N_W (or N_P) is not a good scaling parameter. The $\langle K^+\rangle / \langle \pi^+\rangle$ ratio for central collisions of small systems is larger, especially at lower energies, than the ratio for peripheral collisions of large systems with the same number of wounded nucleons $\langle N_W\rangle$. This may be due to low collision density in peripheral reactions.

The $\langle K^-\rangle / \langle \pi^-\rangle$ ratio, not shown here, behaves qualitatively similar to the $\langle K^+\rangle / \langle \pi^+\rangle$ ratio.

ϕ-mesons:

The ϕ vector meson has zero net strangeness and is not expected to be correlated to total strangeness production if it is produced according to the statistical hadron gas model. However if the ϕ is produced by coalescence of a strange and an anti-strange quark its yield will be sensitive to the strange quark density of the produced matter.

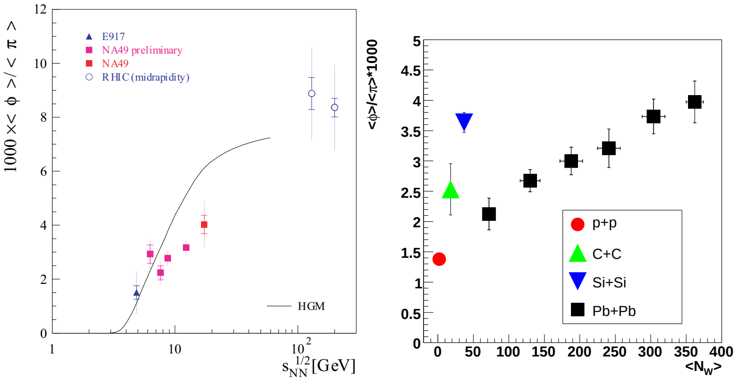

FIGURE 4. Left: Energy dependence of the $\langle \phi\rangle / \langle \pi\rangle$ ratio for central Pb+Pb (Au+Au) collisions [13, 14]. Right: System size dependence of the $\langle \phi\rangle / \langle \pi\rangle$ ratio at 158*A* GeV [9, 15].

The energy dependence of the $\langle \phi\rangle / \langle \pi\rangle$ ratio (figure 4) shows indications of a non-monotonic behavior at the low SPS energies. The system size dependence shows a similar structure as it was observed for the $\langle K^+\rangle / \langle \pi^+\rangle$ ratio. This indicates that ϕ production is sensitive to total strangeness production and favors the picture of the ϕ production via coalescence of a strange and an anti-strange quark.

Hyperons:

The energy dependence of the $\langle \Lambda\rangle / \langle \pi\rangle$ ratio shows a maximum at high AGS or low SPS energies. The position of that maximum is consistent with the position of the maximum in the $\langle K^+\rangle / \langle \pi^+\rangle$ ratio. The energy dependence of $\langle \Lambda\rangle / \langle \pi\rangle$ can be approximately reproduced by a hadron gas model assuming $\gamma_S = 1$ [16] (see solid curve in figure 5). The $\langle \Xi\rangle / \langle \pi\rangle$ ratio seem to have a maximum at low SPS energies like the $\langle K^+\rangle / \langle \pi^+\rangle$ and the $\langle \Lambda\rangle / \langle \pi\rangle$ ratios. The maximum is absent in the $\langle \Omega\rangle / \langle \pi\rangle$ ratio. The analysis of multi-strange hyperons is in progress and future results might clarify the situation.

Both the $\langle \Xi\rangle / \langle \pi\rangle$ and the $\langle \Omega\rangle / \langle \pi\rangle$ ratios at SPS energies are underestimated by the string hadronic UrQMD model [18] (see curves in figure 5).

s and $\bar{\text{s}}$ yield:

The yields of K^-, Λ, Ξ and Ω were used to calculate the total number of constituent s-

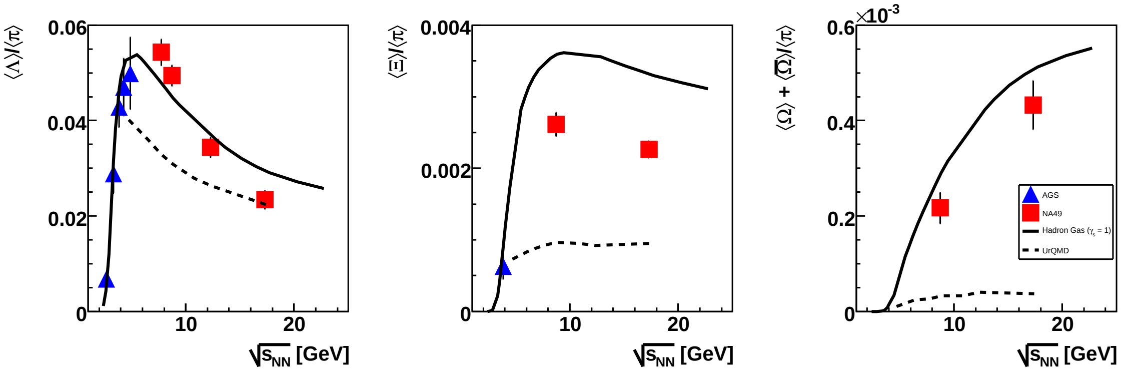

FIGURE 5. Energy dependence of the $\langle\Lambda\rangle/\langle\pi\rangle$ [9, 14], $\langle\Xi\rangle/\langle\pi\rangle$ [14] and $\langle\Omega+\bar{\Omega}\rangle/\langle\pi\rangle$ [17] ratios in central Pb+Pb (Au+Au) collisions.

quarks produced in the reaction. The corresponding antiparticles were used to estimate the $\bar{\text{s}}$-quark yield. The correction for the missing measurements was calculated based on the hadron gas model [19].

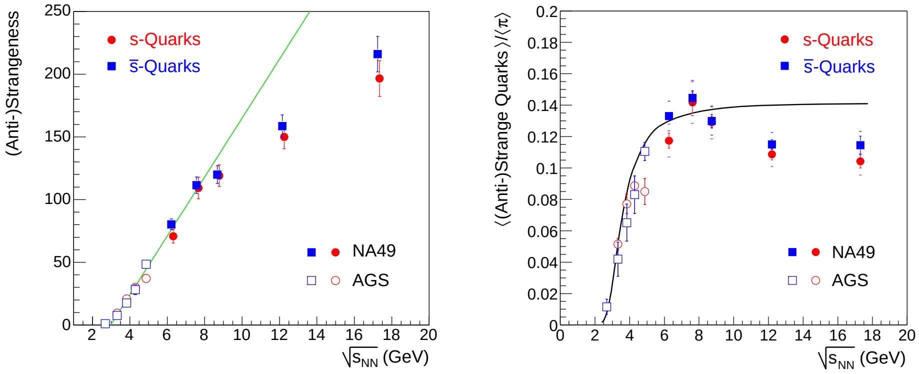

FIGURE 6. Energy dependence of constituent s and $\bar{\text{s}}$ quark multiplicities (left) and their ratios to the pion yield (right).

Figure 6 shows that both NA49 and AGS data fulfill strangeness conservation ($\langle \text{s}\rangle = \langle\bar{\text{s}}\rangle$). The "horn" which was observed in the $\langle K^{+}\rangle/\langle\pi^{+}\rangle$ ratio is also seen in the $\langle s\rangle/\langle\pi\rangle$ and $\langle\bar{s}\rangle/\langle\pi\rangle$ ratios. The energy dependence of $\langle \text{s}\rangle$ and $\langle\bar{\text{s}}\rangle$ also shows an anomaly at low SPS energies: the increase of strangeness with energy is getting weaker at the low SPS energies.

Transverse mass spectra:

The transverse mass spectra can be parametrized by the inverse slope parameter T obtained by fitting the function $d^2n/(m_T dy dm_T) = C\cdot\exp(-(m_T)/\text{T})$. Collective flow effects cause a flattening in the low $m_T - m_0$ domain for heavier particles whereas at high $m_T - m_0$ the particle spectra follow rather a power law than an exponential dependence. Thus the fit range has to be limited to an intermediate m_T range. A simple exponential parametrization works best for kaons.

Another characterization of the shape of transverse mass spectra is the mean transverse mass $\langle m_T \rangle$. Its advantage is that it can be used even for non-exponential spectra.

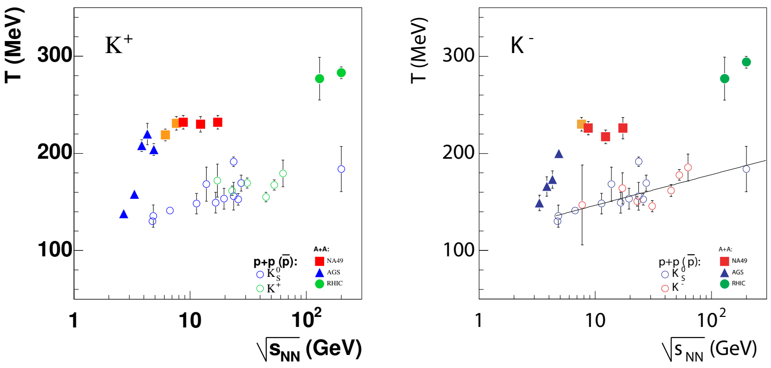

FIGURE 7. Energy dependence of the inverse slope parameter of kaons for central Pb+Pb (Au+Au) and p+p [20] collisions.

Figure 7 shows that the inverse slope parameter of kaons increases in the AGS and RHIC energy domains but it stays constant at SPS energies. This feature, which is not seen in p+p interactions, might be attributed to the latent heat of a phase transition [5] and is in fact consistent with hydrodynamic model calculations assuming a first order phase transition [21].

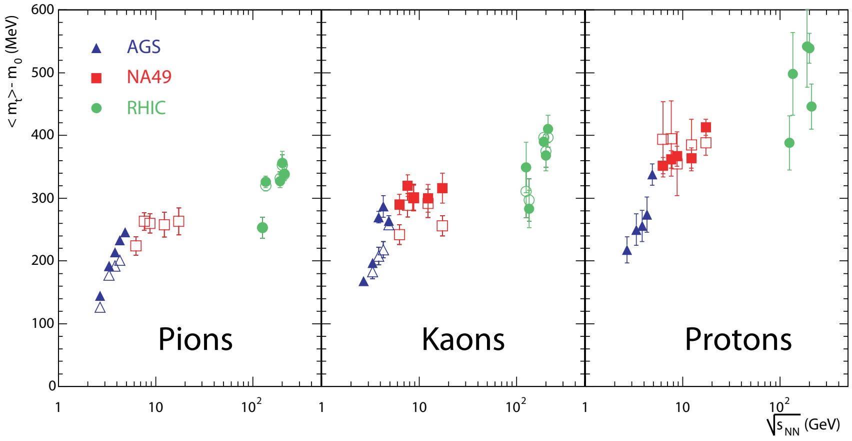

FIGURE 8. Energy dependence of the mean transverse mass of various hadrons produced in central Pb+Pb (Au+Au) collisions. Positive (negative) particles are represented by full (open) symbols.

Similar energy dependence (the "step") is evident from figure 8 for $\langle m_T \rangle - m_0$. It seems to be present for pions, kaons and protons.

The inverse slope parameter T fitted in the intermediate m_T region rises linearly with particle mass with the slope being larger for larger systems (figure 9). This effect could be explained in the following way: The inverse slope has both a thermal component and a contribution of the collective expansion. The latter gets larger for heavier particles and larger colliding systems.

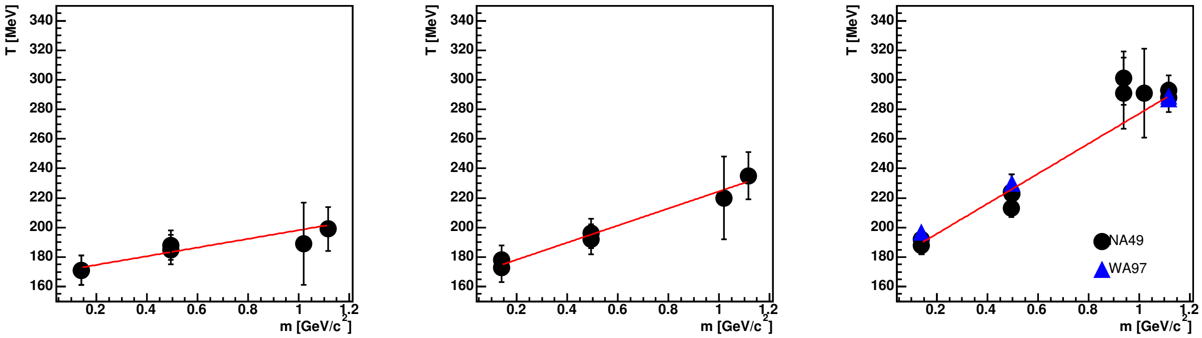

FIGURE 9. Mass dependence of the inverse slope parameter in central C+C, Si+Si [9] and Pb+Pb [4, 22] collisions at 158*A* GeV.

CONCLUSION

Several anomalies in the energy dependence of hadron production properties were observed by the NA49 experiment. These are the "kink" for pion multiplicities, the "horn" for the strangeness to pion ratio and the "step" for the mean transverse mass of various hadrons. These observations can not be described by present hadronic models. In contrast, the results are consistent with the onset of deconfinement at low SPS energies [5, 23].

The system size dependence of various hadronic observables, e.g. the $\langle K \rangle / \langle \pi \rangle$ ratio, shows early saturation in central collisions of different size nuclei. Peripheral collisions of large nuclei behave quite differently from central collisions of small nuclei with the same number of wounded nucleons. This difference is larger for smaller energies.

Acknowledgements: This work was supported by the US Department of Energy Grant DE-FG03-97ER41020/A000, the Bundesministerium fur Bildung und Forschung, Germany, the Virtual Institute VI-146 of Helmholtz Gemeinschaft, Germany, the Polish State Committee for Scientific Research (1 P03B 097 29, 1 PO3B 121 29, 2 P03B 04123), the Hungarian Scientific Research Foundation (T032648, T032293, T043514), the Hungarian National Science Foundation, OTKA, (F034707), the Polish-German Foundation, the Korea Research Foundation Grant (KRF-2003-070-C00015) and the Bulgarian National Science Fund (Ph-09/05).

REFERENCES

1. F. Karsch, E. Laermann, and A. Peikert, *Nucl. Phys.* **B605**, 579–599 (2001), `hep-lat/0012023`.
2. Z. Fodor, and S. D. Katz, *JHEP* **04**, 050 (2004), `hep-lat/0402006`.
3. S. Afanasev, et al., *Nucl. Instrum. Meth.* **A430**, 210–244 (1999).
4. M. Gazdzicki, et al., *J. Phys.* **G30**, S701–S708 (2004), `nucl-ex/0403023`.
5. M. Gazdzicki, and M. I. Gorenstein, *Acta Phys. Polon.* **B30**, 2705 (1999), `hep-ph/9803462`.
6. M. Gazdzicki, and D. Roehrich, *Z. Phys.* **C65**, 215–223 (1995).
7. J. L. Klay, et al., *Phys. Rev.* **C68**, 054905 (2003), `nucl-ex/0306033`.

8. P. Dinkelaker, *J. Phys.* **G31**, S1131–S1136 (2005).
9. C. Alt, et al., *Phys. Rev. Lett.* **94**, 052301 (2005), `nucl-ex/0406031`.
10. J. Bachler, et al., *Nucl. Phys.* **A661**, 45–54 (1999).
11. F. Wang, *J. Phys.* **G27**, 283–300 (2001), `nucl-ex/0010002`.
12. S. Hamieh, K. Redlich, and A. Tounsi, *Phys. Lett.* **B486**, 61–66 (2000), `hep-ph/0006024`.
13. S. V. Afanasev, et al., *Phys. Lett.* **B491**, 59–66 (2000).
14. V. Friese, *J. Phys.* **G31**, S911–S918 (2005), `nucl-ex/0412013`.
15. V. Friese, *Nucl. Phys.* **A698**, 487–490 (2002).
16. J. Cleymans, and K. Redlich, *Phys. Rev.* **C60**, 054908 (1999), `nucl-th/9903063`.
17. C. Alt, et al., *Phys. Rev. Lett.* **94**, 192301 (2005), `nucl-ex/0409004`.
18. S. A. Bass, et al., *Prog. Part. Nucl. Phys.* **41**, 225–370 (1998), `nucl-th/9803035`.
19. F. Becattini, M. Gazdzicki, A. Keranen, J. Manninen, and R. Stock, *Phys. Rev.* **C69**, 024905 (2004), `hep-ph/0310049`.
20. M. Kliemant, B. Lungwitz, and M. Gazdzicki, *Phys. Rev.* **C69**, 044903 (2004), `hep-ex/0308002`.
21. M. Gazdzicki, et al., *Braz. J. Phys.* **34**, 322–325 (2004), `hep-ph/0309192`.
22. F. Antinori, et al., *Eur. Phys. J.* **C14**, 633–641 (2000).
23. J. Letessier, and J. Rafelski (2005), `nucl-th/0504028`.